Chemistry and Physics of Lipids 221 (2019) 193–197

Contents lists available at ScienceDirect

Chemistry and Physics of Lipids

journal homepage: www.elsevier.com/locate/chemphyslip

Steroid–steroid interactions in biological membranes: Cholesterol and cortisone

Adree Khondker[a,b], Jochen S. Hub[c], Maikel C. Rheinstädter[a,b,*]

[a] Department of Physics and Astronomy, McMaster University, Hamilton, Ontario, Canada
[b] Origins Institute, McMaster University, Hamilton, Ontario, Canada
[c] Theoretical Physics and Center for Biophysics, Saarland University, Saarbrücken, Germany

ARTICLE INFO

Keywords:
Cortisone
Lipid bilayers
Cholesterol
Steroid flare
X-ray diffraction
Molecular dynamics simulations

ABSTRACT

Steroid flares are common side effects associated with corticosteroid treatment, and have been recently theorized to be a consequence of drug crystallization. It was previously reported that the lipid bilayer can promote crystallization of cortisone at high local concentrations. Here, we studied the effect of cholesterol on this membrane induced cortisone crystallization. By combining x-ray diffraction and Molecular Dynamics simulations we observe that that the presence of cholesterol suppresses cortisone-induced membrane thinning and cortisone transnucleation. Cortisone located in the head-tail interface of the membranes also in the presence of cholesterol. The cholesterol molecules were found to be tilted and displaced towards the bilayer center as function of cortisone concentration, away from their canonical position. Our results show that membrane cholesterol may play an important role in the ability of lipid bilayers to catalyze the formation of corticosteroid crystallites.

1. Introduction

Cortisone (17-hydroxy-11-dehydrocorticosterone) is a synthetic corticosteroid used globally as an immunosupressant. Cortisone is commonly used to treat local joint inflammation by direct injection to the active site, and primarily acts by binding to an intracytoplasmic nuclear receptor, ultimately leading to the inhibition of inflammation-inducing prostaglandins (Barnes et al., 1993). As a steroid molecule, cortisone-membrane interactions can be observed both *in-vivo* and *in-vitro* and may play a role in their respective mechanisms of action. (Arrowsmith et al., 1983; Shlatz and Marinetti, 1972).

There are, however, several severe side-effects of cortisone, which include muscle wasting, hyperglycemia, and steroid psychosis (Schäcke et al., 2002; Buchman, 2001). Many of these side-effects are partially explained by non-specific interactions between the drug and off-targets. One major consequence of the intra-articular injection of cortisone is the onset of a “steroid flare” reaction (Zhou et al., 2012; Goldfarb et al., 2007). These are characterized by acute post-injection pain at the site of administration and typically occur over 1-2 days of injection. One leading theory is that high local concentrations of cortisone lead to the formation of insoluble, micrometer sized crystals that form upon the synovial membrane and cause macrophages to collect at the site of crystallization (Berthelot et al., 2013). The subsequent immune response is thought to give rise to the steroid flare.

Comprehensive MD simulations have shed light on steroid–membrane interactions, providing atom-function relationships that determine partitioning, conformation, and kinetics for these interactions (Atkovska et al., 2018). It is well understood that the interactions between small molecules and biological membranes can offer insights into nonspecific drug side-effects and disease progression (Pabst et al., 2010; Alsop et al., 2014; Khondker et al., 2017).

We have previously reported that cortisone crystallization occurs in unsaturated lipid bilayers made of 1-palmitoyl-2-oleoyl-sn-glycero-3-phosphocholine (POPC) at high cortisone concentrations (Alsop et al., 2016). Membranes were found to thin with increasing cortisone concentration and Bragg peaks due to cortisone crystallization were observed at 35 mol% cortisone. Cholesterol is present at high concentrations in most biological membranes. Because of cholesterol's high affinity to the hydrophobic membrane core and its property to stabilize membrane structure, it can be speculated to have a significant impact on membrane-cortisone interactions. Surface pressure studies using lipid monolayers have indeed suggested that membrane cholesterol offered resistance to hydrocortisone penetration (Cleary and Zatz, 1977).

Herein, we report on the interactions between cortisone and cholesterol-enriched POPC membranes. The presence of cortisone was

* Corresponding author.
E-mail address: rheinstadter@mcmaster.ca (M.C. Rheinstädter).

https://doi.org/10.1016/j.chemphyslip.2019.04.003
Received 11 December 2018; Received in revised form 27 March 2019; Accepted 1 April 2019
Available online 03 April 2019
0009-3084/

found to lead to continuous thinning of the bilayers; however, cortisone crystallites were not observed to form at high cortisone concentrations. The location of cortisone within the bilayer is found to be within the lipid head groups at both low and high concentrations, gradually increasing the cholesterol tilt with increasing cortisone concentration. These results suggest that membrane cholesterol inhibits the insertion and transnucleation of cortisone into lipid bilayers, thus suppressing the formation of cortisone crystallites in model membranes.

2. Materials and methods

2.1. X-ray diffraction

Highly-oriented multi-lamellar membranes were prepared on polished single-side silicon wafers. 1-palmitoyl-2-oleoyl-sn-glycero-3-phosphocholine, (POPC, Avanti Polar Lipids), cholesterol (Avanti) and cortisone (Sigma) were mixed at the desired molecular ratio and dissolved in 1:1 chloroform (Caledon)/2,2,2-trifluoroethanol (TFE) (Sigma). The solutions were deposited on the wafers and annealed, as described in (Alsop et al., 2016). Out-of-plane and in-plane x-ray scattering data was obtained using the Biological Large Angle Diffraction Experiment (BLADE) at McMaster University. BLADE uses a 9 kW (45 kV, 200 mA) CuKα rotating anode at a wavelength of 1.5418 Å. Both source and detector are mounted on moveable arms such that the membranes stay horizontal during measurements. Focussing, multi layer optics provide a high intensity collimated, 200 µm sized beam with monochromatic x-ray intensities up to 10^8 counts/s. Scattering was detected using a Rigaku HyPix-3000 2D semiconductor detector with an area of 3000 mm^2 and 100 µm pixel size, as described previously (Khondker et al., 2018).

By using highly-oriented stacks, the in-plane ($q_{\|}$) and out-of-plane (q_z) structure of the membrane can be decoupled. Using a 2-dimensional detector, both vectors are scanned simultaneously. All scans were measured in the membranes' fluid phase at a temperature of 301 K and 97% relative humidity (RH) (Mills et al., 2008).

The relative electron density, ρ(z), is approximated by one-dimensional Fourier analysis,

$$\rho(z) = \frac{2}{d_z}\sum_{n=1}^{N}\sqrt{I_n q_n}\,v_n \cos\left(\frac{2\pi n z}{d_z}\right), \quad (1)$$

where N is the highest order Bragg peak observed in the experiment. The integrated peak intensities, I_n, are multiplied by q_n to receive form factors, $F(q_n)$. The bilayer form factor $F(q_z)$, which is in general a complex quantity, is real-valued in the case of centro-symmetry. The phase problem of crystallography, therefore, simplifies to the sign problem $F(q_z) = \pm |F(q_z)|$ and the phases, v_n, can only take the values ± 1. The phases are needed to reconstruct the electron density profile from the scattering data following Eq. (1). When the membrane form factor $F(q_z)$ is measured at several q_z values, a continuous function, $T(q_z)$, which is proportional to $F(q_z)$, can be fitted to the data:

$$T(q_z) = \sum_n \sqrt{I_n q_n}\,\mathrm{sinc}\left(\frac{1}{2}d_z q_z - \pi n\right). \quad (2)$$

The analytical expression for $T(q_z)$ has been determined from fitting the experimental peak intensities, a phase array of v_n = [-1 -1 1 -1 1] was used for all membrane samples (Alsop et al., 2016).

2.2. Molecular dynamics simulations

The membrane system consisted of 128 to 160 lipids with 5000 water molecules and varying amount of cortisone, as described in Table 1. Lipid interactions were described by the SLipids forcefield (Jämbeck and Lyubartsev, 2012), and TIP3P water model was used (Mark and Nilsson, 2001). All MD simulations were performed using the GROMACS 4.6 software package (Abraham et al., 2015). Each simulation system was constructed with the MemGen web server (http://memgen.uni-goettingen.de) (Knight and Hub, 2015). Cortisone was described by the General Amber Force Field and taken from a previous study (Alsop et al., 2016). All simulations used a 2 fs time step, with periodic boundary conditions. Electrostatic interactions were computed with the particle-mesh Ewald method, using a direct-space cutoff at 1.2 nm (Darden et al., 1993). Dispersion interactions and short-range repulsion were described together by a Lennard–Jones potential with a cutoff at 1.2 nm. Verlet pair-lists were updated every 10 fs. The SETTLE algorithm was used to constrain the geometry of water molecules(Miyamoto and Kollman, 1992), and LINCS was used to constrain all other bonds (Hess et al., 1997). The temperature was controlled using a Nose–Hoover thermostat at 27 °C (τ = 0.5 ps) (Evans and Holian, 1985), and a semi-isotropic Parrinello-Rahman barostat was used to maintain a pressure at 1 bar (τ = 1 ps) (Parrinello and Rahman, 1981). An overview of all systems prepared for the MD simulations is shown in Table 1. Equilibrium systems were simulated for 200 ns each. All analyses were performed with the final 20 ns of the simulations (unless stated otherwise).

Table 1
Summary of all systems prepared for the MD simulations. The POPC to cholesterol ratio was held at 7:3.

System	$n_{POPC+Cholesterol}$	$n_{Cortisone}$	Simulation time (ns)	$n_{replicate}$
1	128	0	400	1
2	128	3	200	1
3	160	40	200	1
4	130	70	200	2
5	100	100	200	1

2.3. Umbrella sampling simulations

The potential of mean force (PMF) for cortisone translocation across a membrane of pure POPC was taken from a previous study (Alsop et al., 2016). The PMF for cortisone in POPC with approx. 30 mol% cholesterol was computed with a similar setup. Briefly, the system contained 68 POPC, 30 cholesterol, and 5390 water molecules. A spacing of 0.1 nm between adjacent umbrella windows was used. Each window was simulated for 100 ns, where the first 10 ns were omitted for equilibration. The PMFs were computed with the WHAM method, as implemented in the g_wham software (Kumar et al., 1992; Hub et al., 2010). First, a non-cyclic PMF was computed, which was (i) reasonably symmetric and (ii) showed only a small offset of 4 kJ/mol between the two bulk water regimes, suggesting that the PMF was converged. Next, a cyclic PMF was computed and symmetrized around the membrane center. More technical details were described previously (Alsop et al., 2016).

3. Results

3.1. X-ray scattering

Highly oriented lipid bilayers of POPC enriched with 30 mol% cholesterol were prepared with varying concentrations of cortisone. The experimental setup is shown in Fig. 1(a). Each sample was equilibrated for 3 h and maintained at 97% RH during the measurement. The specular reflectivity across q_z is shown in Fig. 1(b). A single series of Bragg peaks is indicative of well-formed highly-oriented membranes. The highest order Bragg peak observed in these high relative humidity cases was n = 5. The constructed electron density profiles are shown in Fig. 1(c). Difference profiles, Δρ(z), were calculated by subtracting the electron density with cortisone from that of just POPC/30% cholesterol membranes to determine the position of the cortisone molecules in the membranes. An increase in electron density was observed between 14 Å$\leqslant$ z $\leqslant$ 20 Å at low and high cortisone concentrations.

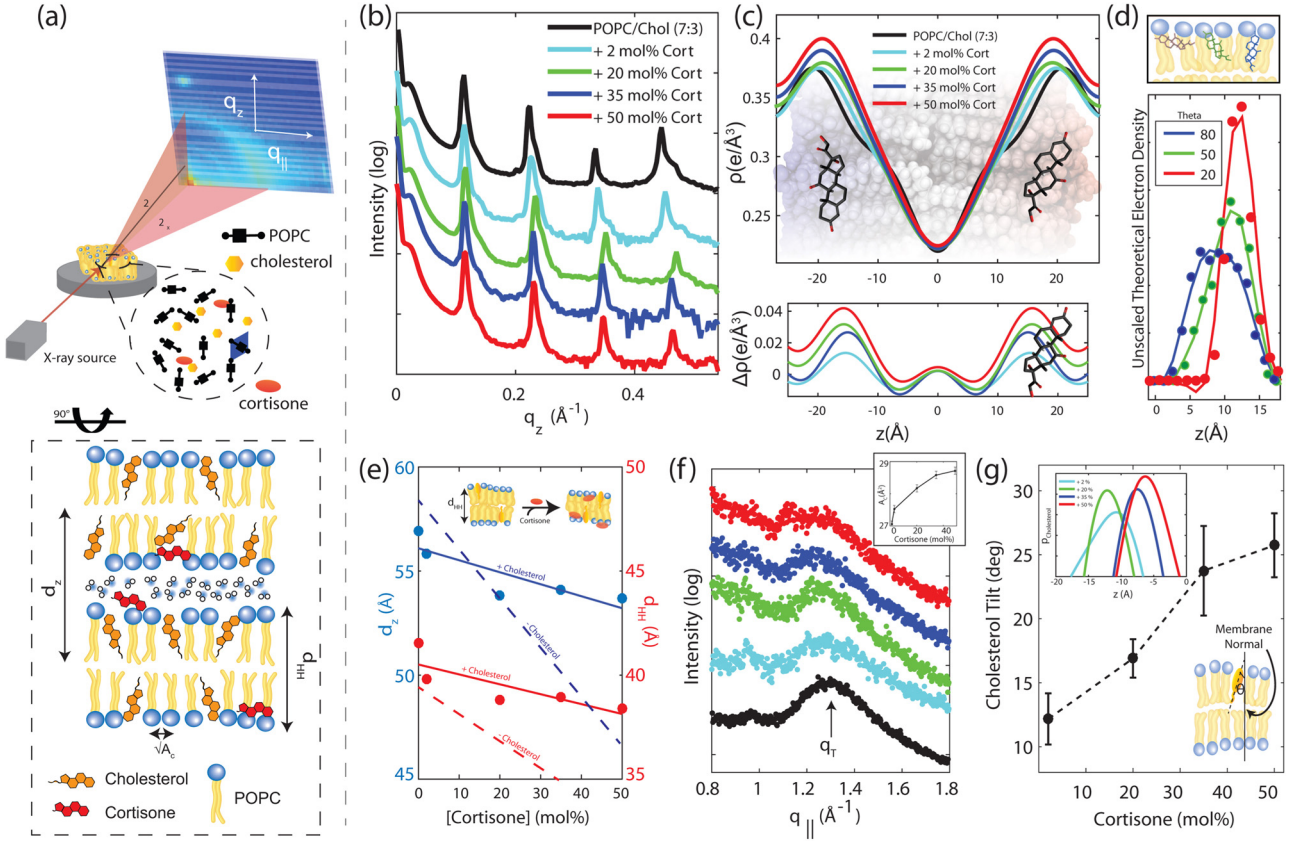

Fig. 1. (a) Experimental setup showing 2D intensity maps from x-ray diffraction, and real-space definitions of d_z, d_{HH}, *and* a_c as described in the Results. (b) Out-of-plane reflectivities of each membrane with varying cortisone concentrations, and (c) calculated electron density profiles with difference profiles between concentration and pure sample, showing cortisone localization in the head-tail interface. (d) Unscaled theoretical electron densities for a single cortisone molecule. (e) Membrane-spacing d_z, and head-head spacing d_{HH}, dashed lines represent slopes from samples without cholesterol (Alsop et al., 2016), (f) In-plane scattering, with indicated tail correlation peak q_T and calculated A_C as function of cortisone concentration. (g) Determined cholesterol tilt angle and cholesterol density as function of cortisone concentration.

To determine the tilt angle of cortisone as a function of cortisone concentration, we first computed the theoretical electron density of a single cortisone molecule at various tilt angles [Fig. 1(d)]. Subsequently, we used least-square fitting of the cortisone tilt angle to the experimentally determined Δρ(z). As shown in Fig. 1(c), the analysis suggests that that cortisone tilts at 10° relative to the bilayer normal within the glycerol group of the lipid bilayers. This angle is held at both low and high concentration regimes.

The lamellar spacing d_z, as determined from the distance of the reflectivity Bragg peaks, and the membrane thickness d_{HH}, as determined from the maxima in the electron density profiles, are plotted in Fig. 1(e). Both, d_z and d_{HH} decrease linearly with increasing cortisone concentration. However, the membrane thinning is significantly smaller as compared to the cholesterol-depleted membranes in (Alsop et al., 2016).

In-plane scattering along $q_{||}$ is shown in Fig. 1(f). The lipid tail correlation peak is observed at $q_{||} \sim 1.32$ Å^{-1} for POPC/cholesterol (7:3 mol/mol) and decreases in $q_{||}$ with increasing cortisone concentration. The lipid tail-tail distance, a_c, was calculated from $a_c = 4\pi/\sqrt{3}q_T$ (Armstrong et al., 2013). From this, the area-per-acyl-chain, A_C can be calculated by using $A_C = \sqrt{3}/2a_L^2$. As shown in the subplot within Fig. 1(f), A_C increases with the cortisone concentration. In cortisone-enriched samples, small in-plane features are noted at q_z-values of 0.8 Å^{-1} < q_z < 1.0 Å^{-1} which may be indicative of the formation of cortisone crystallites upon or within the bilayer as previously reported (Alsop et al., 2016).

The average position and tilt of cholesterol molecules was determined by subtracting the electron density of POPC/Cortisone from POPC/Cholesterol/Cortisone to isolate $\rho_{cholesterol}$ (Alsop et al., 2016). We solved the electron density of 30 mol% cholesterol in the membrane and used a similar fitting procedure to that of cortisone to determine the molecular tilt, as shown in Fig. 1(g). With increasing cortisone concentration, the cholesterol tilt was found to increases with respect to the bilayer normal. By determining the center-of-mass from the cholesterol electron densities, it was observed that with increasing tilt angle, the cholesterol molecules also move closer to the bilayer center.

3.2. Molecular dynamics simulations

The experiments were complemented by all-atom MD simulations. Snapshots of simulations at each concentration are shown in Fig. 2(a), while the mass density of cortisone and cholesterol are presented in Fig. 2(b). Irrespective of the cortisone concentration, and in qualitative agreement with the experimental findings, the cortisone density peak remains at the head-to-tail interface, where the amphiphilic cortisone molecule may form both polar and apolar contacts. However, the position of the coritsone density peak was slightly shifted towards the membrane center, indicative of membrane thinning [Fig. 2(b), top] (Fig. 3).

In contrast, cholesterol molecules were found to displace towards the bilayer center with increasing cortisone content, away from their in a canonical position [Fig. 2(b), bottom]. Cholesterol tilt was computed from the tilt of the sterol backbone with respect to the bilayer normal over the last 5 ns of simulation [Fig. 2(c)]. Evidently, the individual tilt of cholesterol molecules in the lipid bilayer increase with increasing cortisone concentration.

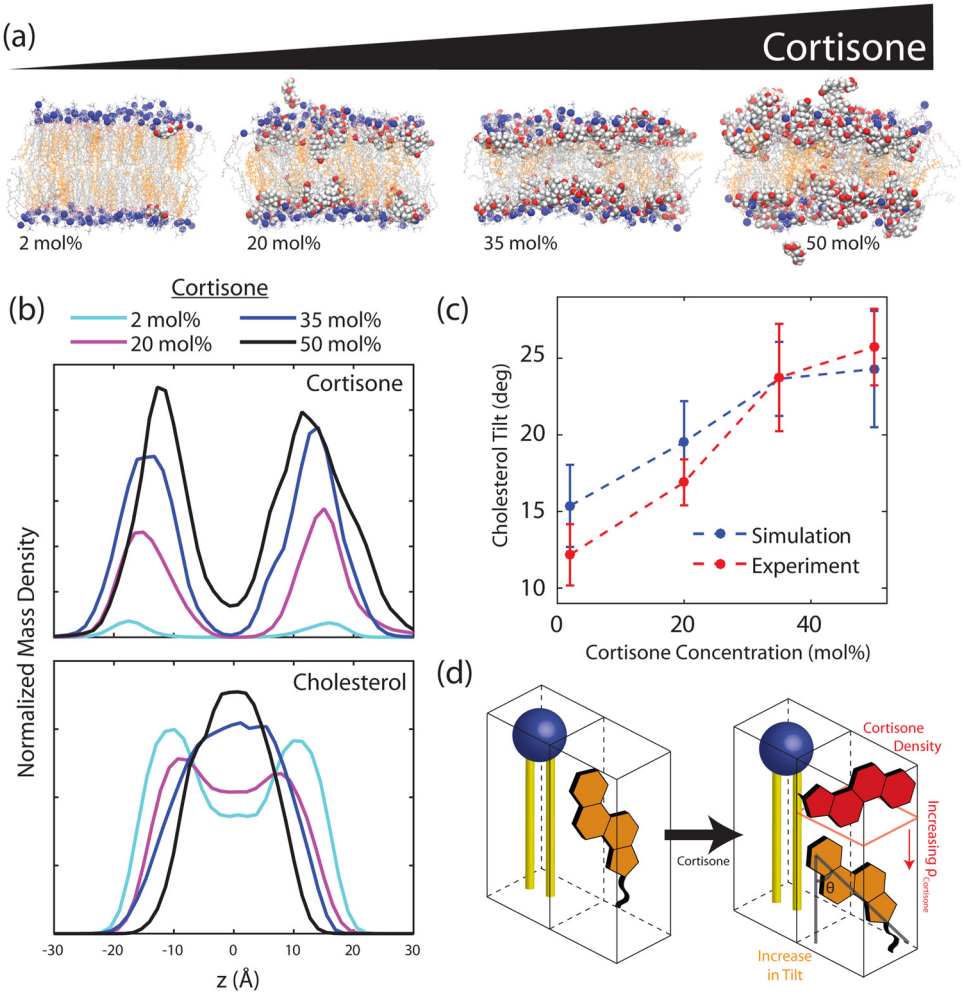

Fig. 2. (a) MD snapshots of 2, 20, 35, and 50 mol% cortisone simulations, cholesterol is shown in orange, and phosphate heads in blue. (b) Relative mass densities of cortisone and cholesterol in POPC bilayers at varying cortisone concentrations from MD simulations. (c) Cholesterol tilt at varying cortisone concentrations from both simulation and experiment. (d) Schematic for cortisone-driven cholesterol tilting in lipid bilayers.

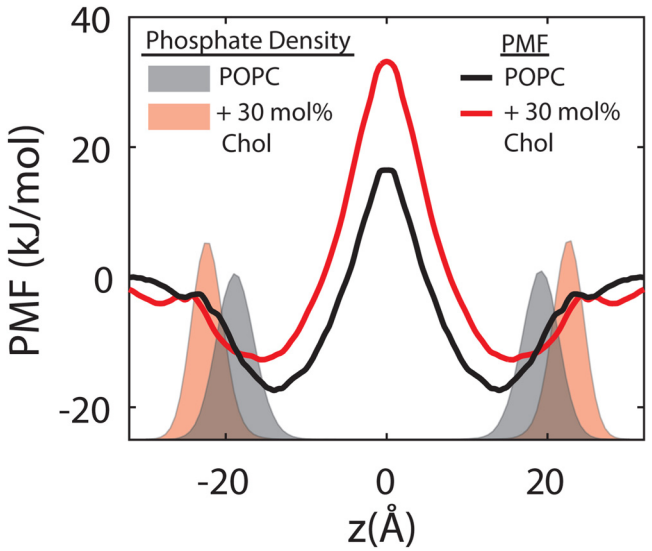

Fig. 3. The PMF profiles for cortisone in both cholesterol-enriched membranes and cholesterol-depleted membranes (Alsop et al., 2016) are shown by line. The average phosphate density from simulation is also shown.

To rationalize the membrane partitioning of cortisone in energetic terms, we computed the potential of mean force (PMF) of cortisone along the membrane normal either for a pure POPC membrane or for a POPC/cholesterol (7:3) membrane. Note that these PMFs were computed with single cortisone molecules in the membrane, hence they reveal cortisone partitioning in the low-concentration limit of cortisone. In line with the density profiles in Fig. 2(b), the PMFs demonstrate that cortisone partitions at the head-to-tail interface at $z \sim \pm 15$ Å, as evident from the pronounced minima in the PMFs. The addition of cholesterol has two effects on the PMF. First, the minima (corresponding the preferred cortisone position) are shifted to larger $|z|$, reflecting a thickening of the membrane. Second, the PMF minima become more shallow, indicating a reduced partitioning of cortisone into cholesterol containing membranes.

4. Discussion

A membrane-bound state of cortisone was observed in the head-tail interface of lipid bilayers at low and high concentrations of cortisone. This position is rationalized by the amphiphilic nature of cortisone. The simulations demonstrate PMF minima for the cortisone across the bilayer, with a strong preference for localization in the glycerol region of the lipid bilayer in membranes with and without cholesterol. Cortisone-induced membrane thinning was found to be significantly reduced due to the presence of cholesterol.

The presence of cortisone had a significant impact on the position of cholesterol molecules within the bilayers. With increase in cortisone concentrations, the cholesterol tilt increased by ~10° and cholesterol molecules were observed to penetrate the bilayer center. The occupancy of cortisone in the head-tail interface likely reduces the free volume for cholesterol within the bilayer, thereby causing cholesterol to exhibit a non-canonical localization. The increasing cortisone density may force this increase in tilt, which correlates with the experimentally determined cholesterol tilt with increasing drug concentration (as pictured in Fig. 2(d)).

Importantly, cortisone transnucleates were not observed in cholesterol-enriched bilayers. As cholesterol is known to decrease the area-per-chain of most membranes and increase bilayer rigidity, cortisone penetration and rotation within the lipid bilayer is expected to be significantly compromised. In pure POPC membranes, inserted cortisone molecules prompted membrane collapse and transnucleation catalyzed the formation of cortisone crystallites with lattice constants of 7.31 Å × 7.31 Å× 22 Å (Alsop et al., 2016). The absence of these sharp Bragg peaks in the in-plane x-ray data in the presence of cholesterol is indicative that cholesterol-enriched membranes are not able to accelerate the formation of cortisone transnucleates.

Cortisone is a commonly used to treat inflammation of the joints as an anti-inflammatory medication. We previously reported that the cortisone may penetrate the bilayer center and promote the formation of cortisone crystallites. Here, we find that membrane cholesterol-cortisone interactions play a significant role in the formation of crystallites. From both experiments and simulations, we find that: (1) the localization of cortisone can force cholesterol molecules to adopt a greater tilt, (2) cortisone partitions in the glycerol region of the bilayer which is further separated in cholesterol-enriched bilayers, (3) cholesterol leads to reduced membrane partitioning of cortisone, and that (4) cholesterol reduces cortisone-induced thinning. Together, these results may shed further light on the initiation of steroid flares and rationalize steroid-steroid interactions.

5. Conclusion

The formation of steroid crystallites has been clinically linked with the onset of steroid flares. In this work, we show that membrane cholesterol can suppress the formation of cortisone crystallites. By combining x-ray diffraction and MD simulations, we provide insights onto the mechanisms of cortisone transnucleation. Cortisone partitions into the head-tail interfacial region of the bilayers at all concentrations of cortisone while displacing membrane cholesterol towards the membrane center with increasing tilt. As cholesterol increases the membrane width, it also decreases the attractive force between cortisone in opposite leaflets, preventing alignment of cortisone and subsequent transnucleation. Cholesterol stabilizes the bilayer preventing membrane collapse and the ability of cortisone to form transmembrane crystallites. These results give rise to a molecular understanding of steroid-steroid interactions in membrane systems.

Acknowledgements

This research was funded by the Canadian Institutes of Health Research (CIHR) Institute of Musculoskeletal Health and Arthritis, Natural Sciences and Engineering Research Council of Canada (NSERC), the Canada Foundation for Innovation (CFI). A.K. is the recipient of a CIHR Summer Studentship Award (Ref. No. 157765) M.C.R. is the recipient of a University Scholar Award from McMaster University. J.S.H. was supported by the Deutsche Forschungsgemeinschaft (HU 1971/4-1).

References

Abraham, Mark James, Murtola, Teemu, Schulz, Roland, Páll, Szilárd, Smith, Jeremy C., Hess, Berk, Lindahl, Erik, 2015. Gromacs: High performance molecular simulations through multi-level parallelism from laptops to supercomputers. SoftwareX 1, 19–25.

Alsop, Richard J., Barrett, Matthew A., Zheng, Songbo, Dies, Hannah, Rheinstädter, Maikel C., 2014. Acetylsalicylic acid (asa) increases the solubility of cholesterol when incorporated in lipid membranes. Soft Matter 10 (24), 4275–4286.

Alsop, Richard J., Khondker, Adree, Hub, Jochen S., Rheinstädter, Maikel C., 2016. The lipid bilayer provides a site for cortisone crystallization at high cortisone concentrations. Sci. Rep. 6, 22425.

Clare L Armstrong, Drew Marquardt, Hannah Dies, Norbert Kučerka, Zahra Yamani, Thad A Harroun, John Katsaras, An-Chang Shi, and Maikel C Rheinstädter, 2013. The observation of highly ordered domains in membranes with cholesterol, PLoS One 8(6), e66162.

Arrowsmith, M., Hadgraft, J., Kellaway, I.W., 1983. The interaction of cortisone esters with liposomes as studied by differential scanning calorimetry. Int. J. Pharmaceut. 16 (3), 305–318.

Atkovska, Kalina, Klingler, Johannes, Oberwinkler, Johannes, Keller, Sandro, Hub, Jochen S., 2018. Rationalizing steroid interactions with lipid membranes: Conformations, partitioning, and kinetics. ACS Central Sci. 4 (9), 1155–1165.

Barnes, Peter J., Adcock, Ian, Spedding, Michael, Vanhoutte, Paul M., 1993. Anti-inflammatory actions of steroids: molecular mechanisms. Trends Pharmacol. Sci. 14 (12), 436–441.

Berthelot, Jean-Marie, Le Goff, Benoît, Maugars, Yves, 2013. Side effects of corticosteroid injections: What's new? Joint Bone Spine 80 (4), 363–367.

Buchman, Alan L., 2001. Side effects of corticosteroid therapy. J. Clin. Gastroenterol. 33 (4), 289–294.

Cleary, Gary W., Zatz, Joel L., 1977. Interaction of hydrocortisone with model membranes containing phospholipid and cholesterol. J. Pharmaceut. Sci. 66 (7), 975–980.

Darden, Tom, York, Darrin, Pedersen, Lee, 1993. Particle mesh Ewald: An N! log (N) method for Ewald sums in large systems. J. Chem. Phys. 98 (12), 10089–10092.

Evans, Denis J., Holian, Brad Lee, 1985. The Nose–Hoover thermostat. J. Chem. Phys. 83 (8), 4069–4074.

Goldfarb, Charles A., Gelberman, Richard H., McKeon, Kathleen, Chia, Ben, Boyer, Martin I., 2007. Extra-articular steroid injection: early patient response and the incidence of flare reaction. J. Hand Surg. 32 (10), 1513–1520.

Hess, Berk, Bekker, Henk, Berendsen, Herman J.C., Fraaije, Johannes GEM, et al., 1997. Lincs: a linear constraint solver for molecular simulations. J. Comput. Chem. 18 (12), 1463–1472.

Hub, Jochen S., de Groot, Bert L., van der Spoel, David, 2010. g_wham-A free weighted histogram analysis implementation including robust error and autocorrelation estimates. J. Chem. Theory Comput. 6, 3713–3720.

Jämbeck, Joakim P.M., Lyubartsev, Alexander P., 2012. Derivation and systematic validation of a refined all-atom force field for phosphatidylcholine lipids. J. Phys. Chem. B 116, 3164–3179.

Khondker, Adree, Alsop, Richard J., Dhaliwal, Alexander, Saem, Sokunthearath, Moran-Mirabal, Jose M., Rheinstädter, Maikel C., 2017. Membrane cholesterol reduces polymyxin b nephrotoxicity in renal membrane analogs. Biophysical Journal 113 (9), 2016–2028.

Khondker, Adree, Malenfant, Dylan J., Dhaliwal, Alexander K., Rheinstädter, Maikel C., 2018. Carbapenems and lipid bilayers: Localization, partitioning, and energetics. ACS Infect. Dis. 4 (6), 926–935.

Knight, Christopher J., Hub, Jochen S., 2015. Memgen: A general web server for the setup of lipid membrane simulation systems. Bioinformatics 31 (17), 2897–2899.

Kumar, S., Bouzida, D., Swendsen, R.H., Kollman, P.A., Rosenberg, J.M., 1992. The weighted histogram analysis method for free-energy calculations on biomolecules. I. The method. J. Comput. Chem. 13, 1011–1021.

Mark, Pekka, Nilsson, Lennart, 2001. Structure and dynamics of the Tip3p, SPC, and SPC/E water models at 298 K. J. Phys. Chem. A 105 (43), 9954–9960.

Mills, Thalia T., Toombes, Gilman E.S., Tristram-Nagle, Stephanie, Smilgies, Detlef-M., Feigenson, Gerald W., Nagle, John F., 2008. Order parameters and areas in fluid-phase oriented lipid membranes using wide angle x-ray scattering. Biophys. J. 95 (2), 669–681.

Miyamoto, S., Kollman, P.A., 1992. SETTLE: An analytical version of the SHAKE and RATTLE algorithms for rigid water models. J. Comp. Chem. 13, 952–962.

Pabst, G., Kučerka, N., Nieh, M.-P., Rheinstädter, M.C., Katsaras, J., 2010. Applications of neutron and x-ray scattering to the study of biologically relevant model membranes. Chem. Phys. Lipids 163 (6), 460–479.

Parrinello, Michele, Rahman, Aneesur, 1981. Polymorphic transitions in single crystals: A new molecular dynamics method. J. Appl. Phys. 52 (12), 7182–7190.

Schäcke, Heike, Döcke, Wolf-Dietrich, Asadullah, Khusru, 2002. Mechanisms involved in the side effects of glucocorticoids. Pharmacol. Therap. 96 (1), 23–43.

Shlatz, L., Marinetti, G.V., 1972. Hormone-calcium interactions with the plasma membrane of rat liver cells. Science 176 (4031), 175–177.

Zhou, Yong, Cho, Kwang-Jin, Plowman, Sarah J., Hancock, John F., 2012. Nonsteroidal anti-inflammatory drugs alter the spatiotemporal organization of ras proteins on the plasma membrane. J. Biol. Chem. 287 (20), 16586–16595.